Enhanced proton beams from ultrathin targets driven by high contrast laser pulses

Neely, D.; Foster, P.; Robinson, A.; Lindau, Filip; Lundh, Olle; Persson, Anders; Wahlström, Claes-Göran; McKenna, P.

Published in:
Applied Physics Letters

DOI:
10.1063/1.2220011

2006

Enhanced proton beams from ultrathin targets driven by high contrast laser pulses

D. Neely, P. Foster, A. Robinson, F. Lindau, O. Lundh et al.

Citation: Appl. Phys. Lett. **89**, 021502 (2006); doi: 10.1063/1.2220011
View online: http://dx.doi.org/10.1063/1.2220011
View Table of Contents: http://apl.aip.org/resource/1/APPLAB/v89/i2
Published by the American Institute of Physics.

Enhanced proton beams from ultrathin targets driven by high contrast laser pulses

D. Neely,[a] P. Foster, and A. Robinson
Central Laser Facility, Rutherford Appleton Laboratory, Chilton, Didcot, Oxon OX11 0QX, United Kingdom

F. Lindau, O. Lundh, A. Persson, and C.-G. Wahlström
Department of Physics, Lund Institute of Technology, P.O. Box 118, S-221 00 Lund, Sweden

P. McKenna
SUPA, Department of Physics, University of Strathclyde, Glasgow G4 0NG, United Kingdom

(Received 14 March 2006; accepted 22 May 2006; published online 13 July 2006)

The generation of proton beams from ultrathin targets, down to 20 nm in thickness, driven with ultrahigh contrast laser pulses is explored. The conversion efficiency from laser energy into protons increases as the foil thickness is decreased, with good beam quality and high efficiencies of 1% being achieved, for protons with kinetic energy exceeding 0.9 MeV, for 100 nm thick aluminum foils at intensities of 10^{19} W/cm^2 with 33 fs, 0.3 J pulses. To minimize amplified spontaneous emission (ASE) induced effects disrupting the acceleration mechanism, exceptional laser to ASE intensity contrasts of up to 10^{10} are achieved by introducing a plasma mirror to the high contrast 10 Hz multiterawatt laser at the Lund Laser Centre. It is shown that for a given laser energy on target, regimes of higher laser-to-proton energy conversion efficiency can be accessed with increasing contrast. The increasing efficiency as the target thickness decreases is closely correlated to an increasing proton temperature. © *2006 American Institute of Physics*.
[DOI: 10.1063/1.2220011]

Significant progress has recently been made in the production of low-divergence beams of MeV protons from the interaction between short pulse, high intensity laser radiation, and thin target foils. Such laser-driven ion beams will potentially find numerous uses in the fields of physics, materials science, and medicine.[1,2] However, important work remains, for example, to increase the maximum proton energy and to optimize the laser-to-proton energy conversion efficiency. Studies along these lines are presently the focus of many research programs worldwide.

The main mechanism behind the highest energy protons is target normal sheath acceleration[3] (TNSA) at the rear surface. In particular, with a hydrogen containing layer on the target surface, always present under the vacuum conditions normally available for laser-plasma experiments, the dominant accelerated ion species is proton, due to their high charge to mass ratio. The highest electron density at the rear surface, and consequently highest acceleration field, is expected for ultrathin targets of a conducting material. As the target thickness is decreased, transverse spreading of the hot electrons inside the target is reduced, resulting in a higher rear surface charge density.[4] In addition, if the thickness is less than $\tau c/2$ (τ is the laser pulse duration and c the speed of light), electron recirculation within the target during the laser pulse may further enhance the acceleration field at the rear surface.[5] Finally, for very high intensities and ultrathin targets, relativistic transparency allows part of the laser pulse to be transmitted through the target and contribute to increased electron heating.[6] However, there are limits to this decrease in target thickness in order to optimize proton acceleration. The most severe limiting factor in experiments is the presence of laser prepulses or a pedestal of amplified spontaneous emission (ASE), affecting the conditions on the target rear surface prior to the arrival of the main laser pulse.[7,8] An induced density gradient can drastically reduce the effectiveness of the TNSA mechanism.[9] The thinner the target, the more sensitive it is to such prepulses. For a given peak laser intensity, the optimum target thickness is thus related to the laser temporal contrast, defined as the ratio between the intensity of the main pulse to that of the pedestal or prepulse. Most experiments reported in the literature are limited to targets with thickness in the range from a few micrometers to several tens of micrometers.

Previous investigations using medium contrast Ti: sapphire laser systems,[4,10] have demonstrated a gradual increase in maximum proton energy observed E_{max} as the target thickness was decreased. For example, Kaluza *et al.* with a laser contrast of 10^7 demonstrate an increase in proton energy with decreasing target thickness down to 2 μm. The increase was attributed to reduced transverse spreading of the hot electrons inside the target. Mackinnon *et al.*,[5] using a laser with a contrast of 10^{10}, demonstrated significant enhancement in E_{max} as the target thickness was decreased below $\tau c/2$ ($\sim$10 μm in their case). This increase was attributed to electron recirculation. In the studies by Kaluza *et al.*,[4] the same drastic enhancement was not observed, possibly because ASE induced density gradients of the target rear surface disrupted the proton acceleration before the recirculation mechanism became effective.

Motivated by these earlier studies we embark on a program of work examining proton acceleration from surface contamination layers on ultrathin target substrates. In particular, we study the influence of target thickness on the laser-to-proton energy conversion efficiency and energy distribution. In this letter we report results with Al targets and ultrahigh contrast laser pulses, allowing us to extend the in-

[a]Electronic mail: d.neely@rl.ac.uk

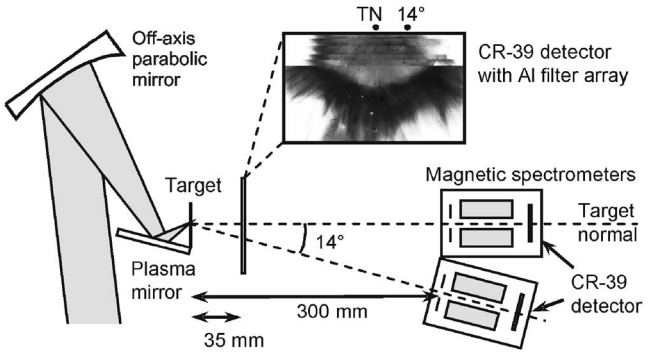

FIG. 1. Schematic of the experimental arrangement showing the plasma mirror geometry and proton diagnostics. The spatial profile monitor only sampled the lower portion of the beam, enabling the magnetic spectrometers situated in the horizontal plane to be operated simultaneously. The inset shows the spatial profile data from a 50 nm foil shot, corresponding to the star in Fig. 2. A filter mask consisting of strips of Al foil with different thicknesses, each stopping protons below a threshold energy, gives a staircase energy response in the vertical direction for the spatial profile.

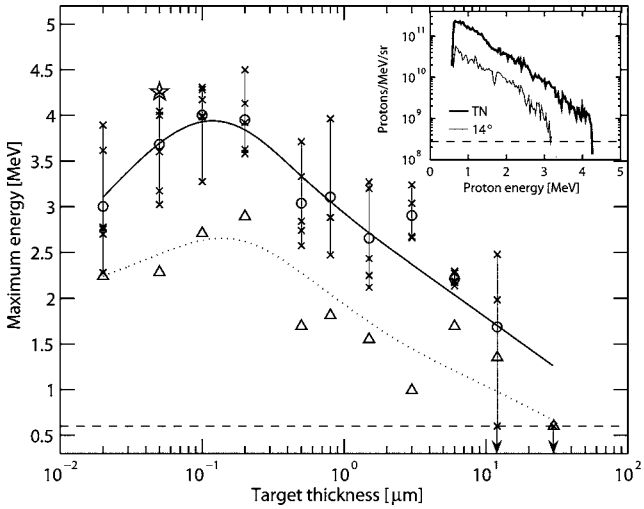

FIG. 2. Maximum proton energies obtained as a function of Al target thickness for on-target contrasts of 10^{10} (crosses). The solid line is a trend line fitted to the on-axis average for each thickness (circles). The 14° average data are represented by the triangles and the dotted trend line. The dashed line represents the detection limit. The inset shows typical proton spectra for the shot represented by the star symbol.

vestigations to significantly thinner targets than previously reported.

The experiment employs the 10 Hz, 800 nm multiterawatt laser system at the Lund Laser Centre (LLC),[7] which delivers 33 fs pulses with a 1 ns duration ASE, at an intensity contrast of 2×10^8. When this laser is focused to an intensity of $\sim10^{19}$ W/cm^2, the ASE pedestal typically launches an ~8 μm/ns shock wave into Al target foils.[7,8] Therefore, to drive targets thinner than 1 μm, contrasts $>10^8$ (or pedestals of much shorter duration) are necessary to maintain an undisturbed target rear surface. To achieve such conditions in the present study we use a plasma mirror.[11] The transition from low to high reflectivity of a plasma mirror can be set to occur as the main pulse rises out of the ASE background approximately a few tens of picosecond before the peak of the pulse. The ASE pedestal is thus transmitted, resulting in a significant increase in temporal contrast in the reflected part of the pulse. Previous plasma mirror studies[12] have demonstrated that it is possible to obtain high contrast and high reflectivity without adding any phase errors by carefully selecting the appropriate irradiance conditions.

We operate our uncoated glass plasma mirror at 45° angle of incidence, in a *P*-polarized geometry, 3 mm from the laser focus. At this point the ASE intensity onto the plasma mirror is always below 10^8 W/cm^2, while the peak laser pulse intensity exceeds 10^{15} W/cm^2. In this configuration we measure a reflectivity of $41\pm3\%$. The contrast enhancement, calculated as the ratio of ASE reflectivity to main pulse reflectivity, is 45 under these conditions leading to an on-target contrast of 10^{10}. The laser pulse is focused onto thin Al foils at 30° angle of incidence by an $f/3$, off-axis parabolic mirror, via the plasma mirror, as illustrated in Fig. 1. With a pulse energy, after the plasma mirror, of 0.3 J and a $1/e^2$ focal spot diameter of 10 μm, the peak intensity on target reaches 10^{19} W/cm^2. In this configuration, and with an ASE contrast of 1×10^{10}, a data set comprising of over 50 shots is obtained for a wide range of target thickness, enabling trends to be clearly identified. The rear surface proton beam emission is sampled by three diagnostics, two magnetic spectrometers operating at deflection angles $\phi=0°$ and 14° with respect to target normal, and a half beam "spatial profile monitor"[8] consisting of a CR-39 track detector covered with an array of Al filters.

Proton spectra from Al foils in the range of 20 nm–30 μm are recorded and a typical example of the 0° and 14° emissions is shown in the inset in Fig. 2. The maximum detectable proton energy (E_{max}) is plotted as a function of target thickness in Fig. 2. The average E_{max} for a given foil thickness increases from 0.6 MeV with 30 μm thick foils to 4 MeV with 0.1 μm and then decreases slightly to 3 MeV for 0.02 μm thickness targets. The shot-to-shot variations under nominally identical conditions at a given foil thickness have an average standard deviation of 12%. It is believed that this is partly due to variation within the proton contamination layer or intensity modulations within the focal spot and will be studied in future experiments.

Proton acceleration using the same incident energy on target but at a lower contrast of 5×10^7 reveals that E_{max} is always lower when using the lower contrast pulse, although comparable for targets thicker than a few micrometers.

The proton spectra show an almost single temperature Boltzmann-like distribution (see inset in Fig. 2.). The number of protons/MeV/Sr, $N(E,\phi)$, can be fitted by a simple distribution of the form $N(E,\phi)=N_0(\phi)\exp[-E/T(\phi)]$, where E is the proton energy in MeV, $N_0(\phi)=N(0,\phi)$ extrapolated from the data to $E=0$, and $T(\phi)$ is the temperature in MeV of the distribution. A plot of the fitted temperatures as a function of target thickness is shown in Fig. 3. The data clearly show an increase in the effective temperature of the protons as the target thickness decreases, with the temperature rising from 0.2 MeV at 12 μm to a maximum temperature of 0.65 MeV for targets of thickness of 0.1 μm and then falling to 0.4 MeV for 0.02 μm targets. $N_0(0)$ is approximately independent of target thickness with an average value of 10^{12} protons/MeV/Sr.

The 14° proton spectra follow similar trends to the target normal data in terms of temperature in the majority of shots. However, in a small number of shots (3 out of 50) an off-axis peaked energy spectrum was observed. The angular divergence of the proton beams generally decreases with increasing proton energy, with the ratio $E_{max}(0)/E_{max}$ (14°) having an average of 1.5 and a standard deviation of 0.4. This ratio

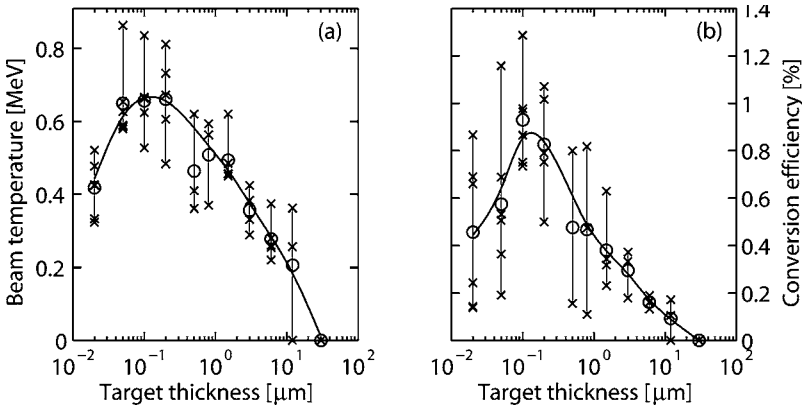

FIG. 3. The effective temperature (a) and energy conversion efficiency to protons with $E>0.9$ MeV (b) of the proton distribution as a function of target thickness. Both curves show maxima for targets of ~100 nm thickness.

does not show any correlation with target thickness. The energy of the energetic part of the proton beam is obtained by integrating the proton beam angular distribution spectrally and spatially for $E>0.9$ MeV, corresponding to the detection threshold of the spatial profile monitor. The beam profile is obtained for each shot by combining the data from the two spectrometers and the spatial profile monitor using cubic spline interpolation. Dividing by the incident drive energy gives the efficiency of conversion into energetic protons, as shown in Fig. 3. The energy transferred into protons of energy above 0.9 MeV increases rapidly with decreasing target thickness and reaches an optimum of ~1% for submicron targets.

Although $N_0(0)$ and divergence show no systematic trends with target thickness, the maximum observed proton energy and beam efficiency exhibit clear trends. The number of accelerated protons increases by approximately a factor of 10 and their average energy also increases as the targets are thinned. It is believed that increasing rear surface hot electron temperatures and densities are enabling these higher proton beam temperatures to be achieved using thinner targets. The observed dependence of E_{max} on target thickness may have different origins in different ranges of thickness. Above a few micrometers, the increase in E_{max} with a decrease in thickness might be dominated by geometrical effects with a decrease in transverse spreading of the hot electrons during transit through the target, as observed by Kaluza *et al.*.[4] Due to the higher contrast available, the thickness can be decreased to even thinner targets in the present study, and we reach a regime where transverse spreading should be negligible. Here E_{max} continues to increase, possibly due to an increasing role of recirculation with decreasing target thickness.[5] It is not expected that self-induced transparency and electron heating by the transmitted fraction of the laser pulse[6] play a significant role at these intensities. Below about 100 nm, we find a decrease in E_{max}, resulting in a clear optimum in thickness. This decrease could be due to the finite temporal contrast on the picosecond time scale, given by the shoulders of the main pulse rather than to ASE or separate prepulses. Establishing the relative contributions of the different effects, including recirculation, refluxing, conduction, and return current inhibitions will be undertaken in future experimental and theoretical studies.

In conclusion, a laser-to-proton beam energy conversion efficiency of 1%, for protons with $E>0.9$ MeV, is obtained for the first time with a short pulse Ti:sapphire laser and pulse energy as low as 0.3 J on target. With a contrast of 10^{10}, the optimum target thickness is found to be as thin as 100 nm. The results show a significant enhancement in proton beam scaling with a variation in target thickness and clearly demonstrate the benefits of using an ultrahigh contrast laser to drive thin targets.

This work was supported by the Access to Research Infrastructures under the Sixth EU Framework Programme contract (RII3-CT-2003-506350, Laserlab Europe), by the Swedish Research Council and the UK Council for the Central Laboratories of the Research Councils.

[1] S. V. Bulanov, T. Z. Esirkepov, V. S. Khoroshkov, A. V. Kunetsov, and F. Pegoraro, Phys. Lett. A **299**, 240 (2002).
[2] M. Roth, E. Brambrink, P. Audebert, M. Basko, A. Blazevic, R. Clarke, J. Cobble, T. E. Cowan, J. Fernandez, J. Fuchs, M. Hegelich, K. Ledingham, L. G. Logan, D. Neely, H. Ruhl, and M. Schollmeier, Plasma Phys. Controlled Fusion **47**, B841 (2005).
[3] S. C. Wilks, A. B. Langdon, T. E. Cowan, M. Roth, M. S. Singh, S. P. Hatchett, M. H. Key, D. M. Pennington, A. J. Mackinnon, and R. A. Snavely, Phys. Plasmas **8**, 542 (2001).
[4] M. Kaluza, J. Schreiber, M. I. K. Santala, G. D. Tsakiris, K. Eidmann, J. Meyer-ter-Vehn, and K. J. Witte, Phys. Rev. Lett. **93**, 045003 (2004).
[5] A. J. Mackinnon, Y. Sentoku, P. K. Patel, D. W. Price, S. P. Hatchett, M. H. Key, C. Andersen, R. A. Snavely, and R. R. Freeman, Phys. Rev. Lett. **88**, 215006 (2002).
[6] E. d'Humiere, E. Lefebvre, L. Grémillet, and V. Malka, Phys. Plasmas **12**, 062704 (2005).
[7] F. Lindau, O. Lundh, A. Persson, P. McKenna, K. Osvay, D. Batani, and C.-G. Wahlström, Phys. Rev. Lett. **95**, 175002 (2005).
[8] P. McKenna, F. Lindau, O. Lundh, D. Neely, A. Persson, and C.-G. Wahlström, Philos. Trans. R. Soc. London, Ser. A **364**, 711 (2006).
[9] A. J. Mackinnon, M. Borghesi, S. P. Hatchett, M. H. Key, P. K. Patel, H. Campbell, A. Schiavi, R. A. Snavely, S. C. Wilks, and O. Willi, Phys. Rev. Lett. **86**, 1769 (2001).
[10] I. Spencer, K. W. D. Ledingham, P. McKenna, T. McCanny, R. P. Singhal, K. Krushelnick, E. L. Clark, P. A. Norreys, R. J. Clarke, D. Neely, A. J. Langley, E. J. Divall, C. H. Hooker, and J. R. Davies, Phys. Rev. E **67**, 046402 (2003).
[11] G. Doumy, F. Quere, O. Gobert, M. Perdrix, Ph. Martin, P. Audebert, J.-C. Gauthier, J.-P. Geindre, and T. Wittmann, Phys. Rev. E **69**, 026402 (2004).
[12] C. Ziener, P. S. Foster, E. J. Divall, C. H. Hooker, M. H. R. Hutchinson, A. J. Langley, and D. Neely, J. Appl. Phys. **93**, 768 (2003).